

3-(4-Phenoxyphenyl)pyrazoles: A Novel Class of Sodium Channel Blockers

Ji Yang,^{*,†} Parviz Gharagozloo,[†] Jiangchao Yao,[†] Victor I. Ilyin,[†] Richard B. Carter,[‡] Phong Nguyen,[§] Silvia Robledo,[§] Richard M. Woodward,[†] and Derk J. Hogenkamp[#]

Discovery Research, Purdue Pharma L.P., 6 Cedar Brook Drive, Cranbury, New Jersey 08512, Novartis Pharmaceuticals Corp., One Health Plaza, East Hanover, New Jersey 07936, Allergan, Inc., 2525 Dupont Drive, Irvine, California 92612, and Department of Pharmacology, College of Medicine, University of California, Irvine, California 92697

Received October 3, 2003

A series of 3-(4-phenoxyphenyl)-1*H*-pyrazoles were synthesized and characterized as potent state-dependent sodium channel blockers. A limited SAR study was carried out to delineate the chemical requirements for potency. The results indicate that the distal phenyl group is critical for activity but will tolerate lipophilic ($+\pi$) electronegative ($+o$) substituents at the ortho and/or para position. Substitution at the pyrazole nitrogen with a H-bond donor improves potency. Compound **18** showed robust activity in the rat Chung neuropathy paradigm.

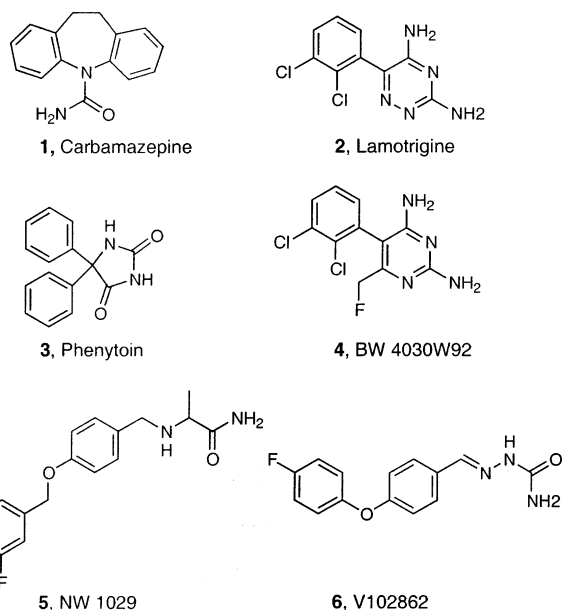
Introduction

Neuropathic pain syndromes are caused by injury to the nervous system. The injury can result from metabolic disorders, infection, or physical trauma. Examples include painful diabetic neuropathy, postherpetic neuralgia (shingles), complex regional pain syndrome, and chronic postoperative pain.^{1,2} A significant proportion (~10%) of lower back pain is also thought to have a neuropathic component.³ Neuropathic pain is chronic in nature and is characterized by allodynia, hyperalgesia, and hyperpathia.⁴ The molecular mechanisms underlying these pain states remain unclear, and treatment options are limited.⁵

A common feature of peripheral neuropathic pain is pathological firing patterns in primary afferent neurons, including ectopic discharge.⁶ There is now a growing body of evidence that voltage-gated Na⁺ channels play a role in establishing and maintaining these firing patterns.^{7,8} In particular, the expression of various Na⁺ channel subunits in primary afferent neurons changes in animal models of nerve injury and neuropathic pain.^{9–12} Furthermore, nociception is modified in animal studies where specific Na⁺ channel subunits have been knocked out or where expression has been decreased by use of intrathecal antisense.^{13,14} It is not surprising, therefore, that drugs such as carbamazepine (**1**), lamotrigine (**2**), and phenytoin (**3**), which block Na⁺ channel function, have shown clinical efficacy in the treatment of neuropathic pain (Chart 1).^{15,16} Still, these compounds were developed as anticonvulsants and are only weakly active at Na⁺ channels. Subsequent efforts to optimize the Na⁺ channel potencies have led to more agents (e.g., **4** and **5**) with improved efficacies in models of inflammatory and neuropathic pain.^{17,18}

V102862 (**6**) is a potent, state-dependent Na⁺ channel blocker that is efficacious in animal models of neuropathic pain. It has a K_i value of ~0.6 μ M on Na currents

Chart 1



in hippocampal neurons, and its MED in the Chung model is ~2.5 mg/kg.^{19–22} An in vivo metabolism study in rats suggested that the semicarbazone moiety of **6** is a major metabolic site leading to the formation of several metabolites.²³ In addition, the compound suffers from poor aqueous solubility. It was envisaged that heterocyclic bioisosteres of the semicarbazone moiety would give analogues with improved metabolic stability and solubility. Our efforts led to compound **10**, where a pyrazole ring was found to be a suitable replacement. In this paper, we report the synthesis of several analogues of **10** with high sodium channel blocking potency.

Chemistry

The procedure for synthesizing the pyrazole series is shown in Scheme 1.^{20,24} Reaction of phenols with 4-fluoroacetophenone gave the desired products in high yields. Subsequent reaction of the phenoxyphenyl ketones with *N,N*-dimethylformamide dimethyl acetal afforded the

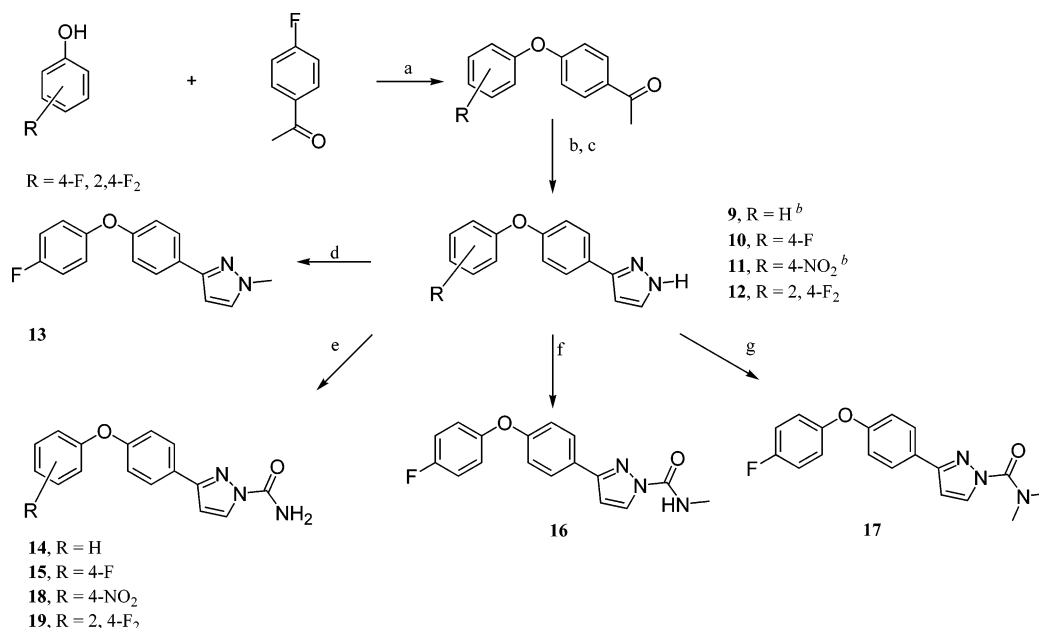
* To whom correspondence should be addressed. Telephone: 609-409-5164. Fax: 609-409-6930. E-mail: ji.yang@pharma.com.

[†] Purdue Pharma L. P.

[‡] Novartis Pharmaceuticals Corp.

[§] Allergan, Inc.

[#] University of California, Irvine.

Scheme 1^a

^a Reagents and conditions: (a) K₂CO₃, DMA, 150 °C; (b) HC(OMe)₂NMe₂, DMF, reflux; (c) hydrazine, EtOH, reflux; (d) MeI, NaOH, *n*-Bu₄NBr; (e) NaOCN, HOAc; (f) methyl isocyanate, CH₂Cl₂; (g) DBU, dimethylcarbonyl chloride, THF. ^b Available commercially.

corresponding β -(dimethylamino)- α,β -unsaturated ketones, which upon treatment with hydrazine–hydrate in ethanol furnished unsubstituted pyrazoles (e.g., **10**). Methylation of **10** with MeI gave **13** in 80% yield. Conversion of the pyrazole intermediates (**9**–**12**) to the respective primary amides **14**, **15**, **18**, and **19** was affected with sodium cyanate in 90% aqueous acetic acid in 50–60% yield. The reaction of **10** with methyl isocyanate or dimethylcarbonyl chloride gave the secondary and tertiary amides **16** and **17**, respectively, in >80% yields.

Results and Discussion

The compounds listed in Table 1 were evaluated in electrophysiological assays for their sodium channel blocking activity. Inhibition of voltage-gated sodium currents was recorded in HEK-293 cells stably expressing hSkM1 sodium channels. The blocking effects of these compounds are generally highly sensitive to the holding voltage, indicating they bind to voltage-sensitive sodium channels in their inactivated states (measured as K_i) and have weaker potency toward resting states (measured as K_r).²⁵

At the inactivated state K_i , a comparison of the structures **7**–**9** reveals that the presence of the distal phenyl group is critical to the potency of the molecules. However, the inclusion of a fluorine atom (present in **6**) in the 4-position of the phenyl group (**10**) has little or no effect on the potency (e.g., compare **9** and **10**, and **14** and **15**). N-methylation of the pyrazole ring (**13**) lowers the potency by about 3-fold, while introduction of a primary amide increases it by about 8-fold. This observation is supported by two comparisons (i.e., **9** and **14**, and **10** and **15**). The results may suggest the requirement of a hydrogen-bond donor in this region of the molecule. This is further supported by the secondary and/or tertiary amide analogues (**16** and **17**) where up to a 10-fold drop in potency results over the primary amide (**15**). Replacement of the fluorine atom in the para

position of the phenyl group with the more lipophilic electron-withdrawing NO₂ group (i.e., **18**) has little effect. Inclusion of a second fluorine atom in the 2-position of the phenyl ring (i.e., **19**) does not change potency.

As mentioned earlier, V102862 (**6**) is a state-dependent Na⁺ channel blocker with 150-fold selectivity between the inactive (K_i) and resting (K_r) states. The selectivity is important to reduce the liability of producing anesthetic-like “nerve blocks” and disruption of normal sensation. The structural modifications incorporated in compounds **9**, **10**, and **13**–**19** appear to have little effect on the resting state potency and in general follow a similar (albeit less pronounced) SAR trend to that observed at the inactivated state. Thus, the majority of the analogues exhibit good to excellent selectivity between the inactivated and resting states of the channels. Compound **19** is the most potent and state-dependent sodium channel blocker reported to date.

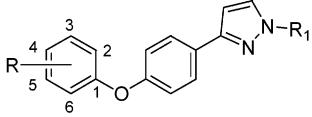
Compound **18** was tested in an experimental model of peripheral neuropathy produced by segmental spinal nerve ligation in the rat (the Chung model, Figure 1) and compared with carbamazepine (**1**).²⁶ The data indicate that **18**, at a dose of 10 mg/kg po, shows robust antiallodynic effects comparable to carbamazepine at 100 mg/kg po across all time points.

Conclusions

3-(4-Phenoxyphenyl)pyrazoles are a novel class of state-dependent sodium channel blockers that have high in vitro potencies. Initially we identified compound **10** to be equipotent to V102862 (**6**). Our SAR results indicate the requirement of a H-bond donor at the pyrazole nitrogen. Finally, at one-tenth of the dose, compound **18** is as efficacious as carbamazepine (**1**) in an in vivo model of neuropathic pain.

Experimental Section

Chemistry. All purchased reagents were used without further purification. Flash chromatography was performed on E. Merck silica gel 60, 230–440 mesh. TLC analysis was

Table 1. In Vitro Potencies at the Inactivated (K_i) and Resting (K_r) States of Sodium Channels^a


Cmpd #	R	R ₁	hSKM1 K _i (μM)	hSKM1 K _r (μM)	R=K _r /K _i
1 Carbamazepine			52±15 (4)	720±240 (6)	14
2 Lamotrigine			17±4 (3)	1440±380 (6)	85
3 Phenytoin			24±5 (4)	620±180 (5)	26
6 V102862			0.18±0.03 (3)	27±10 (6)	150
7^b			61±1 (3)	1110±270 (3)	18
8^b			81±16 (3)	710±140 (3)	9
9	H	H	0.24±0.11 (4)	16±2 (4)	67
10	4-F	H	0.20±0.06 (3)	17±3 (3)	85
13	4-F	Me	0.69±0.18 (3)	21±10 (4)	30
14	H	CONH ₂	0.035±0.007 (3)	5±1 (3)	143
15	4-F	CONH ₂	0.031±0.013 (3)	6±1 (3)	194
16	4-F	CONHMe	0.15±0.04 (4)	21±4 (4)	140
17	4-F	CONMe ₂	0.34±0.01 (3)	26±2 (3)	76
18	4-NO ₂	CONH ₂	0.031±0.013 (3)	7±1 (3)	226
19	2,4-F ₂	CONH ₂	0.025±0.015 (3)	10±5 (3)	400

^a The potencies were measured on the human skeletal muscle hSkM1 Na⁺ cell line (hosted in HEK-293 cells). The K_i and K_r values are the measured potencies at the inactivated and resting states of sodium channels, respectively. The numbers in parentheses are run times. ^b Available commercially.

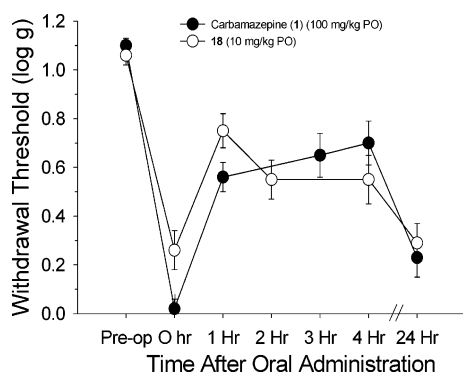


Figure 1. Rat Chung neuropathy test for carbamazepine and **18**: dose- and time-response relation for compound-induced changes in the mechanical force required to produce paw withdrawal in rat (mechanical threshold). The threshold was determined manually on the left plantar surface with von Frey filaments using the up-down method. Neuropathic injury involved tightly ligating the left L5 and L6 spinal nerves. Each point is the mean ± SEM for a group of eight animals. Pre-op represents the preoperative control. The zero time values show the hypersensitivity (allodynia) that developed during the 1 week following surgery.

carried out on a glass plate precoated with silica gel 60 F₂₅₄. Melting points were determined on a MEL-TEMP II capillary melting point apparatus and are uncorrected. ¹H NMR spectra were recorded on a Bruker Avance 400 spectrometer and were referenced to TMS, and all chemical shifts are reported as δ (ppm) values. LC/MS experiments were performed on an

Agilent 1100 series LC/MSD. HRMS experiments were performed on a Bruker Apex II 4.7T FTMS.

3-[4-(4-Fluorophenoxy)phenyl]-1H-pyrazole (10). A mixture of 4-fluoroacetophenone (20 g, 0.14 mol, 1.0 equiv), 4-fluorophenol (17.8 g, 0.16 mol, 1.1 equiv), and potassium carbonate (18 g, 0.13 mol, 0.9 equiv) in *N,N*-dimethylacetamide (80 mL) was heated at 150 °C for 16 h. The mixture was cooled to room temperature, diluted with CHCl₃ (200 mL), and washed with 2 N aqueous sodium hydroxide solution (2 × 100 mL). The organic layer was dried over sodium sulfate, filtered, and evaporated under reduced pressure to afford the crude product (30 g). This was dried in vacuo (40 °C/1 mmHg) for 2 h to give 4-(4-fluorophenoxy)acetophenone as a viscous brown oil (27.5 g, 83%). ¹H NMR (CDCl₃) δ 7.93 (d, *J* = 8.7 Hz, 2H), 7.09–7.04 (m, 4H), 6.96 (d, *J* = 8.4 Hz, 2H), 2.57 (s, 3H).

4-(4-Fluorophenoxy)acetophenone (23 g, 0.1 mol) and *N,N*-dimethylformamide dimethylacetal (13 g, 0.11 mol) in DMF (70 mL) were heated at 150 °C for 16 h. The solution was cooled to room temperature, and water (250 mL) was added over a period of 20 min. The yellow precipitate was collected by filtration, washed with water (3 × 200 mL), and dried in vacuo at 60 °C for 24 h (27 g). The product (5 g, 17.5 mmol) was dissolved in ethanol (70 mL), followed by the addition of 35% aqueous hydrazine (10.0 g, 0.11 mol). The solution was heated at 80 °C for 1.5 h and then taken to dryness. The crude product was redissolved in ethyl acetate and washed with water (2 × 50 mL) and brine (50 mL). The residue was further purified on a silica gel column, eluting with 1:1 EtOAc/hexane to give **10** as an off-white solid (5.3 g, 95%). ¹H NMR (CDCl₃) δ 10.6 (bs, 1H), 7.71 (d, *J* = 8.4, 2H), 7.60 (d, *J* = 2.1 Hz, 1H), 7.04–

6.99 (m, 6H), 6.57 (d, $J = 2.4$ Hz, 1H). HRMS Calcd for $C_{15}H_{11}FN_2O$: 254.0855. Found: 254.0856. Anal. ($C_{15}H_{11}FN_2O$) C, H, N.

3-[4-(4-Fluorophenoxy)phenyl]-1-methyl-1H-pyrazole (13). A mixture of **10** (0.4 g, 1.6 mmol), CH_3I (0.3 g, 2.1 mmol), NaOH (6N, 1 mL), and $n-Bu_4NBr$ (20 mg) in MeOH (4 mL) was stirred at room temperature for 24 h. The mixture was partitioned between EtOAc and water. The organic layer was separated, dried over $MgSO_4$, and concentrated in vacuo. The residue was purified by column chromatography (EtOAc/hexanes 3:7) to afford **13** as a colorless oil (0.32 g, 80%). 1H NMR ($CDCl_3$) δ 7.78 (d, 2H, $J = 8.7$ Hz), 7.39 (d, $J = 2.2$ Hz, 1H), 6.09–7.09 (m, 6H), 6.51 (d, $J = 2.4$ Hz, 1H), 3.96 (s, 3H). HRMS Calcd for $C_{16}H_{13}FN_2O$: 268.1012. Found: 268.1012. Anal. ($C_{16}H_{13}FN_2O$) C, H, N.

3-[4-(4-Fluorophenoxy)phenyl]-1H-pyrazole-1-carboxamide (15). A solution of sodium cyanate (1.4 g, 20.7 mmol) in water (5 mL) was added to a solution of **10** (4.4 g, 17.3 mmol) in 90% aqueous acetic acid (65 mL). The reaction mixture was stirred at room temperature for 16 h. Water was added, and the precipitate was collected by filtration. The residue was chromatographed on silica gel (EtOAc/hexanes 1:1) to give **15** as a white solid (2.79 g, 52%): mp = 141–143 °C; 1H NMR ($DMSO-d_6$) δ 8.28 (d, $J = 3.0$ Hz, 1H), 7.94 (d, $J = 8.7$ Hz, 2H), 7.84 (bs, 2H), 7.24 (t, $J = 8.4$ Hz, 2H), 7.13–7.08 (m, 2H), 7.04 (d, $J = 8.4$ Hz, 2H), 6.94 (d, $J = 2.7$ Hz, 1H). HRMS Calcd for $C_{16}H_{12}FN_3O_2$: 297.0914. Found: 297.0913. Anal. ($C_{16}H_{12}FN_3O_2$) C, H, N.

3-[4-(4-Fluorophenoxy)phenyl]-1H-pyrazole-1-carboxylic Acid Methylamide (16). A solution of **10** (0.4 g, 1.6 mmol) and methyl isocyanate (0.1 g, 1.8 mmol) in CH_2Cl_2 (4 mL) was stirred at room temperature for 24 h. The solvent was removed, and the residue was chromatographed on silica gel (EtOAc/hexanes 3:7) to afford **16** as a colorless oil (0.4 g, 80%). 1H NMR ($CDCl_3$) δ 8.28 (d, $J = 2.6$ Hz, 1H), 7.81 (d, $J = 8.7$ Hz, 2H), 7.15–7.25 (br, 1H), 7.05–7.10 (m, 6H), 6.67 (d, $J = 2.8$ Hz, 1H), 3.09 (d, $J = 5.0$ Hz, 3H). HRMS Calcd for $C_{17}H_{14}FN_3O_2$: 311.1070. Found: 311.1070. Anal. ($C_{17}H_{14}FN_3O_2$) C, H, N.

3-[4-(4-Fluorophenoxy)phenyl]-1H-pyrazole-1-carboxylic Acid Dimethylamide (17). A solution of **10** (0.4 g, 1.6 mmol), DBU (0.4 g), and dimethylcarbonyl chloride (0.25 g, 1.5 mmol) in THF (10 mL) was stirred at room temperature for 24 h. The reaction mixture was partitioned between EtOAc and water. The organic layer was separated, washed with brine, dried over $MgSO_4$, and concentrated. The crude product was chromatographed on silica gel (EtOAc/hexanes 3:7) to afford **17** as a colorless oil (0.42 g, 84%). 1H NMR ($CDCl_3$) δ 8.18 (d, $J = 2.6$ Hz, 1H), 7.82 (d, $J = 8.8$ Hz, 2H), 7.02–7.09 (m, 6H), 6.66 (d, $J = 2.6$ Hz, 1H), 3.24–3.36 (br, 6H). HRMS Calcd for $C_{18}H_{16}FN_3O_2$: 325.1227. Found: 325.1223. Anal. ($C_{18}H_{16}FN_3O_2$) C, H, N.

The syntheses of **14**, **18**, and **19** were carried out following the same experimental procedures that were described for **15**.

3-(4-Phenoxyphenyl)-1H-pyrazole-1-carboxamide (14): mp = 132–133 °C; 1H NMR ($CDCl_3$) δ 8.24 (d, $J = 2.7$ Hz, 1H), 7.80 (d, $J = 8.7$ Hz, 2H), 7.37 (t, $J = 8.4$ Hz, 2H), 7.14 (t, $J = 7.5$ Hz, 1H), 7.08–7.05 (m, 2H), 7.06 (d, $J = 9.0$ Hz, 2H), 6.90 (d, $J = 3.0$ Hz, 1H), 5.30 (bs, 2H). HRMS Calcd for $C_{16}H_{13}N_3O_2$: 279.1008. Found: 279.0998. Anal. ($C_{16}H_{13}N_3O_2$) C, H, N.

3-[4-(4-Nitrophenoxy)phenyl]-1H-pyrazole-1-carboxamide (18): mp = 145–147 °C; 1H NMR ($CDCl_3$) δ 8.28 (d, $J = 2.4$ Hz, 1H), 8.23 (d, $J = 9.0$ Hz, 2H), 7.91 (d, $J = 8.4$ Hz, 2H), 7.16 (d, $J = 8.7$ Hz, 2H), 7.07 (d, $J = 9.3$ Hz, 2H), 6.73 (d, $J = 3.0$ Hz, 1H), 5.3 (bs, 2H). HRMS Calcd for $C_{16}H_{12}N_4O_4$: 324.0859. Found: 324.0861. Anal. ($C_{16}H_{12}N_4O_4$) C, H, N.

3-[4-(2,4-Difluorophenoxy)phenyl]-1H-pyrazole-1-carboxamide (19): mp = 132–134 °C; 1H NMR ($CDCl_3$) δ 8.24 (d, $J = 2.7$ Hz, 1H), 7.79 (d, $J = 8.7$ Hz, 2H), 7.15–7.08 (m, 2H), 6.99 (d, $J = 8.4$ Hz, 2H), 6.94–6.85 (m, 1H), 6.67 (d, $J = 3.0$ Hz, 1H), 5.30 (bs, 2H). HRMS Calcd for $C_{16}H_{11}F_2N_3O_2$: 315.0819. Found: 315.0821. Anal. ($C_{16}H_{11}F_2N_3O_2$) C, H, N.

Biology. Electrophysiology. Cell Culture. The human skeletal muscle Na^+ (hSKM1) cell line (hosted in HEK-293 cells) was a generous gift from Dr. A. L. George, Jr. (Vanderbilt University Medical Center, Nashville, TN). For electrophysiology, cells were plated onto 35 mm Petri dishes (precoated with poly-D-lysine) at a density of $\sim 10^4$ cells/dish on the day of reseeding from confluent cultures. HEK-293 cells were suitable for recordings for 3–4 days after plating.

Patch-Clamp Recordings. Whole-cell voltage-clamp recordings were made using conventional patch-clamp techniques at room temperature (ca. 22 °C).^{27a} The patch-clamp pipettes were pulled from thick-walled borosilicate glass (WPI, Sarasota, FL). Currents were recorded using an Axopatch 200A amplifier (Axon Instruments, Union City, CA) and were leak-subtracted (P/4 or by analog built-in circuitry), low-pass-filtered (3 kHz, 8-pole Bessel), digitized (20–50 μs intervals), and stored using Digidata-1200 B interface and Pclamp8.1/Clampex software (Axon Instruments, Union City, CA). When necessary, residual series access resistance was largely (75–80%) canceled using built-in amplifier circuitry. External solution contained the following (in mM): 150 NaCl, 5.4 KCl, 1.8 $CaCl_2$, 1 $MgCl_2$, 10 D-glucose, 5 HEPES; pH 7.4 (NaOH). The internal solution contained the following (in mM): 130 CsF, 20 NaCl, 1 $CaCl_2$, 2 $MgCl_2$, 10 EGTA, 10 HEPES; pH 7.3 (CsOH). Osmolality was set at ~ 10 mmol/kg lower than that for external solution.

Drug Application. Drug solutions and intervening intervals of wash were applied through a linear array of flow pipes (Drummond Microcaps, 2 μL , 64 mm length). Drugs were dissolved in dimethyl sulfoxide (DMSO) to make 1–30 mM stock solutions. The stock solutions were diluted into external solution to generate final concentrations of 0.003–10 μM . At the highest concentration, the concentration of DMSO was 0.1%. At this level, DMSO itself had only marginal inhibitory effects on the peak Na^+ current.

Stimulation Protocol and Data Analysis. To assess tonic (resting state) block membrane voltage was held at -120 mV at which all hSKM1 Na^+ channels are in the resting state. From this holding voltage, a depolarizing testing pulse to 0 mV was applied to cause maximal sodium current. The size of the current was measured in the control and in the presence of high (3 μM) concentration of an antagonist. The ratio of these amplitudes defined FR (fractional response). The constant, K_r , for inhibition was determined using the following equation (a modified form of the logistic equation with the slope factor $n = 1$):^{27b}

$$K_r = \frac{FR}{1 - FR} [\text{antag}]$$

where [antag] is the concentration of the antagonist used. To measure the affinity toward the inactivated state of the channel, two distinct experimental paradigms were used. For most of the compounds tested, we used depolarizing prepulse protocol. Here, cells again were held at a holding potential of -120 mV to keep nearly all the channels in the closed state. Then a 3 s depolarizing step (“prepulse”) was made to the voltage (usually 0 mV) where the maximum current was elicited. At the end of this depolarization, all the channels would be in the inactivated state. A 3 ms hyperpolarizing step back to -120 mV was then made in order to remove some channels from the inactivated state. These channels comprised the fraction that had no antagonist bound and thus recovered from inactivation caused by the prepulse very rapidly ($> 95\%$ recovery within 2 ms).^{27c} A final depolarizing step (“test pulse”) was used to assay the fraction of sodium channels available for activation. Sodium currents were measured at this test pulse before and after application; FR values were calculated for different concentrations of an antagonist. The latter were used to plot partial concentration inhibition curves. Each individual curve was fitted by the logistic expression

$$\frac{1}{1 + ([\text{antag}]/K_r)^n}$$

using approximation programs within the Origin 5.0 software to get the dissociation constant K_i for inactivated channels. This protocol was applicable only for antagonists that, upon binding to the channel, cause a significant retardation of recovery from inactivation.^{27d} Compounds **7** and **8** did not cause any retardation. To assess their inhibitory effect on inactivated channels, we measured the shift in the midpoint of steady-state inactivation.^{27e} For this aim, double-pulse protocol was used to collect the steady-state inactivation curve. Cells were held at a holding voltage of -120 mV to remove residual steady-state inactivation. A series of 10–12 depolarizing conditioning prepulses (each 3 s in duration) incrementing in 10 mV steps immediately followed by a 5 ms testing pulse to 0 mV were applied at a frequency of $1/7$ s. The peak currents in response to the test pulse were plotted against the size of the corresponding conditioning prepulses to get the steady-state inactivation curve. The Boltzmann fit to this curve, i.e.,

$$\frac{1}{1 + \exp[(V - V_{1/2})/k]}$$

returned the values of $V_{1/2}$ (the half-inactivation voltage) and k (the slope of the curve). These parameters were measured in the control and in the presence of an antagonist. The apparent dissociation constant K_i for binding to the inactivated state was calculated using the modified equation from Bean et al.:^{27e}

$$\frac{[\text{antag}]}{\left[\frac{\exp(-\Delta V_{1/2}/k)}{1 - a} - 1 \right]}$$

where $\Delta V_{1/2}$ is the shift in the midpoint curve (i.e., $\Delta V_{1/2}(\text{antagonist}) - \Delta V_{1/2}(\text{control})$) and a is the normalized inhibition of the current at the most negative end of the inactivation curve. The data are mean \pm SEM with $n = 3-4$.

In Vivo Pharmacology. Chung Methods. Male Sprague–Dawley rats weighing between 150 and 200 g (Harlan Sprague–Dawley, Inc., San Diego, CA) were anesthetized with halothane. The left branches of the L5 and L6 spinal nerves were surgically exposed and tightly ligated with 6.0 silk sutures as previously described. Rats were evaluated prior to surgery and 7–28 days after surgery for the development of tactile allodynia. Manual measurements of tactile sensitivity were performed using von Frey filaments (North Coast Medical), ranging from 3.64 to 5.46/0.6 to 26 g of pressure. Starting with the largest filament, filaments were applied to the plantar surface of the left hind paw with enough force to cause the filament to bend. This force was maintained either until the rat withdrew the limb or for a maximum of 4 s. A positive or “allodynic” response was characterized by a sharp withdrawal of the hind limb that may be followed by flicking or licking of the paw. In the event of a positive response, a thinner filament was applied to the left hind paw as described. A negative response, as characterized by the lack of reaction to the filament, resulted in cessation of testing. This cycle was repeated three times on each rat, and values were expressed as the log gram of force. The mean value of the three measurements was determined for each rat, and the data were expressed as the mean \pm standard error (SEM) for each time point. Allodynic rats were defined as those animals with postsurgical baseline withdrawal thresholds below 0.30 log gram units. Rats were fasted for a minimum of 6 h prior to drug administration. A minimum 48 h washout was allowed for each rat prior to subsequent experimental repetitions. Animals in the vehicle group were administered 1% DMSO and 10% TWEEN-80 po. Drugs were administered orally at a volume of 10 mL/kg body weight. Tactile allodynia measurements were recorded at 1, 2, 4, and 24 h postdrug administration.

Acknowledgment. The authors thank Elena Kutlina for assistance on hSkM1 Na/HEK-293 cell culture

preparation, Zhengrong Xu and Xun Chen for animal surgeries, Leon Zhou for HRMS analysis, and Dr. Ravi Upasani for helpful discussions.

Supporting Information Available: Additional experimental procedures for compound syntheses, electrophysiology, and in vivo pharmacology. This material is available free of charge via the Internet at <http://pubs.acs.org>.

References

- Calcult, N. A. Potential mechanisms of neuropathic pain in diabetes. *Int. Rev. Neurobiol.* **2002**, *50*, 205–228.
- Wasner, G.; Schattschneider, J.; Binder, A.; Baron, R. Complex regional pain syndrome—diagnostic, mechanisms, CNS involvement and therapy. *Spinal Cord* **2003**, *41*, 61–75.
- Argoff, C. E. Pharmacologic management of chronic pain. *J. Am. Osteopath. Assoc.* **2002**, *102* (9, Suppl. 3), S21–S27.
- Zimmermann, M. Pathobiology of neuropathic pain. *Eur. J. Pharmacol.* **2001**, *429*, 23–37.
- Devor, M. Neuropathic pain: what do we do with all these theories? *Acta Anaesthesiol. Scand.* **2001**, *45*, 1121–1127.
- Amir, R.; Michaelis, M.; Devor, M. Burst discharge in primary sensory neurons: triggered by subthreshold oscillations, maintained by depolarizing afterpotentials. *J. Neurosci.* **2002**, *22*, 1187–1198.
- Persaud, N.; Strichartz, G. R. Micromolar lidocaine selectively blocks propagating ectopic impulses at a distance from their site of origin. *Pain* **2002**, *99*, 333–340.
- Wood, J. N.; Akopian, A. N.; Baker, M.; Ding, Y.; Geoghegan, F.; Nassar, M.; Malik-Hall, M.; Okuse, K.; Poon, L.; Ravenall, S.; Sukumaran, M.; Souslova, V. Sodium channels in primary sensory neurons: relationship to pain states. *Novartis Found. Symp.* **2002**, *241*, 159–168 (discussion on pp 168–172 and 226–232).
- Abdulla, F. A.; Smith, P. A. Changes in Na(+) channel currents of rat dorsal root ganglion neurons following axotomy and axotomy-induced autotomy. *J. Neurophysiol.* **2002**, *88*, 2518–2529.
- Craner, M. J.; Klein, J. P.; Renganathan, M.; Black, J. A.; Waxman, S. G. Changes of sodium channel expression in experimental painful diabetic neuropathy. *Ann. Neurol.* **2002**, *52*, 786–792.
- Decosterd, I.; Ji, R. R.; Abdi, S.; Tate, S.; Woolf, C. J. The pattern of expression of the voltage-gated sodium channels Na(v)1.8 and Na(v)1.9 does not change in uninjured primary sensory neurons in experimental neuropathic pain models. *Pain* **2002**, *96*, 269–277.
- Gold, M. S.; Weinreich, D.; Kim, C. S.; Wang, R.; Treanor, J.; Porreca, F.; Lai, J. Redistribution of Na(V)1.8 in uninjured axons enables neuropathic pain. *J. Neurosci.* **2003**, *23*, 158–166.
- Lai, J.; Gold, M. S.; Kim, C. S.; Bian, D.; Ossipov, M. H.; Hunter, J. C.; Porreca, F. Inhibition of neuropathic pain by decreased expression of the tetrodotoxin-resistant sodium channel, NaV1.8. *Pain* **2002**, *95*, 143–152.
- Laird, J. M.; Souslova, V.; Wood, J. N.; Cervero, F. Deficits in visceral pain and referred hyperalgesia in Nav1.8 (SNS/PN3)-null mice. *J. Neurosci.* **2002**, *22*, 8352–8356.
- Dickenson, A. H.; Matthews, E. A.; Suzuki, R. Neurobiology of neuropathic pain: mode of action of anticonvulsants. *Eur. J. Pain.* **2002**, *6* (Suppl. A), 51–60.
- Jensen, T. S. Anticonvulsants in neuropathic pain: rationale and clinical evidence. *Eur. J. Pain.* **2002**, *6* (Suppl. A), 61–68.
- For reviews, see the following. (a) Anger, T.; Madge, D. J.; Mulla, M.; Riddall, D. Medicinal chemistry of neuronal voltage-gated sodium channel blockers. *J. Med. Chem.* **2001**, *44*, 115–137. (b) Banos, J. E.; Sanchez, G.; Berrendero, F.; Maldonado, R. Neuropathic pain: Some clues for future drug treatments. *Mini-Rev. Med. Chem.* **2003**, *3* (7), 719–727.
- (a) Trezise, D. J.; John, V. H.; Xie, X. M. Voltage- and use-dependent inhibition of Na+ channels in rat sensory neurons by 4030W92, a new antihyperalgesic agent. *Br. J. Pharmacol.* **1998**, *124*, 953–963. (b) Veneroni, O.; Maj, R.; Calabresi, M.; Faravelli, L.; Fariello, R. G.; Salvati, P. Anti-allodynic effect of NW-1029, a novel Na+ channel blocker, in experimental animal models of inflammatory and neuropathic pain. *Pain* **2003**, *102*, 17–25. (c) Omana-Zapata, I.; Khabbaz, M. A.; Hunter, J. C.; Bley, K. R. QX-314 inhibits ectopic nerve activity associated with neuropathic pain. *Brain Res.* **1997**, *771*, 228–237. (d) Flippin, L. A.; Lin, X.-F.; Loughhead, D. G.; Weikert, R. J. Phenoxy-methylpiperidine derivatives being sodium channel blockers. European Patent EP 869119, 1998.
- Dimmock, J. R.; Sidhu, K. K.; Thayer, R. S.; Mack, P.; Duffy, M. J.; Reid, R. S.; Quail, J. W.; Pugazhenth, U.; Ong, A.; et al. Anticonvulsant activities of some arylsemicarbazones displaying potent oral activity in the maximal electroshock screen in rats accompanied by high protection indices. *J. Med. Chem.* **1993**, *36*, 2243–2252.

- (20) Dimmock, J. R.; Puthucode, R. N.; Smith, J. M.; Hetherington, M.; Quail, J. W.; Pugazhenti, U.; Lechler, T.; Stables, J. P. (Aryloxy)aryl semicarbazones and related compounds: a novel class of anticonvulsant agents possessing high activity in the maximal electroshock screen. *J. Med. Chem.* **1996**, *39*, 3984–3997.
- (21) Ilyin, V. I.; Whittemore, E. R.; Puthucode, R. N.; Dimmock, J. R.; Woodward, R. M. Co 102862, a novel anticonvulsant, is a potent, voltage-dependent blocker of voltage-gated Na⁺ channels in rat hippocampal neurons. *Soc. Neurosci. Abstr.* **1997**, *23*, 2163.
- (22) Ilyin, V. I.; Woodward, R. M. Kinetic and steady-state parameters for inhibition of hSkM1 sodium channels by Co 102862, phenytoin, carbamazepine and lamotrigine. *Soc. Neurosci. Abstr.* **1998**, *24*, 1939.
- (23) Kumar, R.; Gilbert, N. L.; Helen, H. In Vivo Metabolism and Mass Balance of 4-[4-Fluorophenoxy]benzaldehyde Semicarbazone in Rats. *Drug Metab. Dispos.* **2000**, *28*, 1153–1161.
- (24) (a) Lin, Y.-I.; Lang, S. A., Jr. Novel two-step synthesis of pyrazoles and isoxazoles from aryl methyl ketones. *J. Heterocycl. Chem.* **1977**, *14*, 345–347. (b) Watson, A. A.; House, D. A.; Steel, P. J. Chiral heterocyclic ligands. VIII. Syntheses and complexes of new chelating ligands derived from camphor. *Aust. J. Chem.* **1995**, *48*, 1549–1572. (c) Jean-Claude, B.; Just, G. Synthesis and stability of 5-, 7- and 8-substituted benzo-1,2,3,5-tetrazepin-4-ones. *Heterocycles* **1998**, *48*, 1347–1363. (d) Hoffmann, M. G. A new route to 1,5-disubstituted 4-arylsulfonylpyrazoles by lithiation of 1-methyl-4-arylsulfonylpyrazoles. *Tetrahedron* **1995**, *51*, 9511–9518.
- (25) Butterworth, J. F.; Strichartz, G. R. Molecular mechanisms of local anesthesia: a review. *Anesthesiology* **1990**, *72*, 711–734.
- (26) Kim, S. H.; Chung, J. M. An experimental model for peripheral neuropathy produced by segmental spinal nerve ligation in the rat. *Pain* **1992**, *50*, 355–363.
- (27) (a) Hamill, O. P.; Marty, A.; Neher, E.; Sakmann, B.; Sigworth, F. J. Improved patch-clamp techniques for high-resolution current recording from cells and cell-free membrane patches. *Pfluegers Arch.* **1981**, *391*, 85–100. (b) Leff, P.; Dougall, I. G. Further concerns over Cheng–Prusoff analysis. *TIPS* **1993**, *14*, 110–112. (c) Ilyin, V. I.; Yang, J.; Nguyen, P. X.; Hogenkamp, D. J.; Gharagozloo, P.; Robledo, S.; Woodward, R. M. State-dependent block of voltage-gated sodium channels by 4-phenoxyphenylpyrazoles. *Program No. 579.6-T, 2003 Abstract Viewer/Itinerary Planner*; Society for Neuroscience: Washington, DC, 2003 (CD-ROM). (d) Kuo, C.-C.; Bean, B. P. Slow binding of phenytoin to inactivated sodium channels in rat hippocampal neurons. *Mol. Pharmacol.* **1994**, *46*, 716–725. (e) Bean, P. B.; Cohen, R. J.; Tsien, R. W. Lidocaine block of cardiac sodium channels. *J. Gen. Physiol.* **1983**, *81*, 613–642.

JM030498Q